https://rbgeomorfologia.org.br/
ISSN 2236-5664

Revista Brasileira de Geomorfologia

v. 24, nº 2 (2023)

http://dx.doi.org/10.20502/rbg.v24i2.2265

Research Article

Delineation of terrain features in Demini's Watershed – Setentrional Amazonia using regional geomorphometry

Delineamento de feições de terreno na bacia hidrográfica do Rio Demini – Amazonia Setentrional utilizando geomorfometria regional

Karolina Gameiro Cota Dias[1] e Márcio de Morisson Valeriano [2]

[1] Instituto Nacional de Pesquisas Espaciais, Divisão de Observação da Terra e Geoinformática, São José dos Campos, Brasil. E-mail: karolina.gameiro@gmail.com - ORCID: https://orcid.org/0000-0003-1487-7308

[2] Instituto Nacional de Pesquisas Espaciais, Divisão de Observação da Terra e Geoinformática, São José dos Campos, Brasil. E-mail: marcio.valeriano@inpe.br - ORCID: https://orcid.org/0000-0002-1985-9005

Recebido: 20/07/2022; Aceito: 25/04/2023; Publicado: 26/05/2023

Abstract: The mapping of terrain features relies on the necessity of an object-based approach, which can be related to the constitution of terrain units. The regionalization of land surface parameters enables the assessment of characteristics inside terrain unities and enhances heterogeneity outside these patches. This study presents a classification methodology for hierarchical geomorphometric delineation, using visual and Random Forest (RF) classification in a regionalized dataset of terrain variables, applied in Demini's watershed, north of Amazonia. These variables, calculated by segments derived from multiresolution segmentation, were evaluated in order to identify which had major contributions in RF's classifications. The characterization of features had great correspondence with Environmental Informations Database (BDIA/IBGE) data of geomorphological mapping, used as reference in this work. The Overall Accuracy for RF taxon 1 was 96%, while Taxon 2 Highland and Lowland RF models reached 84% and 87%, respectively. Identification of subdomain classes were possible mostly using the digital elevation model (Topodata DEM) and variables directly derived from the DEM. The delineation of floodplain presented significant differences between visual and RF results, including BDIA's data.

Keywords: Digital Elevation Model; Segmentation; Regionalization; Landform Classification; Machine Learning.

Resumo: O mapeamento de feições de terreno é dependente de uma abordagem baseada em objetos, que pode estar relacionada à constituição de unidades do terreno. A regionalização dos parâmetros geomorfométricos permite a avaliação das características dentro das unidades do terreno e realça a heterogeneidade fora dessas. Este estudo apresenta uma metodologia de classificação para delineamento geomorfométrico hierárquico, usando classificação visual e Random Forest (RF) em um conjunto de variáveis geomorfométricas regionalizadas, aplicado na bacia hidrográfica do rio Demini, norte da Amazônia. Essas variáveis, calculadas em segmentos derivados de segmentação multiresolução, foram avaliadas a fim de identificar quais tiveram maiores contribuições nas classificações de RF. A caracterização das feições teve grande correspondência com os dados de mapeamento geomorfológico do Banco de Dados de Informações Ambientais (BDIA/IBGE), utilizado como referência neste trabalho. A Precisão Geral para o resultado obtido do táxon 1 de RF foi de 96%, enquanto os modelos de Highland e Lowland do Táxon 2 do RF atingiram 84% e 87%, respectivamente. A identificação de classes de subdomínios foi possível principalmente usando o modelo digital de elevação (Topodata DEM) e variáveis diretamente derivadas do DEM. A delimitação da planície de inundação apresentou diferenças significativas entre os resultados visuais e de RF, incluindo os dados do BDIA.

Palavras-chave: Modelo Digital de Elevação, Segmentação, Regionalização, Classificação do relevo, Aprendizado de máquina.

1. Introduction

The mapping of terrain features has been developed in different ways worldwide (CASSETI, 2005). Historically, this procedure has evolved from the point-based localization of most significant physiographic elements to maps containing information about morphometry, genesis, lithology, and even predictions of geomorphological processes (TRICART, 1965).

Regarding morphometry, measuring terrain attributes provides input for many landscape studies and applications (FLORINSKY, 2017). In advance, the availability of automated mapping procedures has increased the number of significant information products. The delineation of urban constructions, such as pavemented streets, pools, and buildings in general, has been improved with object-based image classification (BLASCHKE, 2010). Equivalent progress can be seen in landform identification. The delineation of terrain patterns can achieve high likelihood using segmentation techniques because of the flexibility of inputs and parameters (GERENTE; VALERIANO; MOREIRA, 2018; BORTOLINI; SILVEIRA, 2021). Similarly, machine learning algorithms have been used to identify and predict, in a large amount of data, such as remote sensing products for large areas, physical characterization of remote areas (KARLSON et al., 2019; SIQUEIRA et al., 2022), because of its easily operational characteristics. Machine learning algorithms present interesting potential for geomorphometry by assessing a large number of predictors and outlining the importance of terrain metrics for relief delineation (DING et al., 2016; SIQUEIRA et al., 2022).

The establishment of terrain units is a fundamental step for landform delineation. For its own nature, a landform only can be characterized in opposition to its surroundings, and defined by attributes within its extent. This determines that a landform is understood as an area at least, disabling the direct analyses of single points. In this background, regionalization appears as a way of calculating and attributing statistics to a terrain unit. For regional geomorphometry, the regionalized variable can assume, then, a representation of a descriptive statistic for an area, favoring the characterization of landform as from terrain patches (MINÁR; EVANS, 2008).

For the Amazonian lowlands, much of its terrain couldn't have been delineated at the detail level. It happens because of the difficulty for in-field campaigns – due to its enormous extent, the almost full coverage of forests, which prevents good visualization of terrain, and also lack of previous data: its study has increased only in the past few decades. Another difficulty for geomorphometric mappings in this area is the terrain itself, of predominantly sedimentary nature, which presents low elevation differences and its subtle expression of pattern variations (VALERIANO; ROSSETTI, 2017).

In digital image processing, segmentation algorithms allow the manipulation of parameters in order to adjust the processing to the desired result. In multiresolution segmentation there is a scale parameter, for example, that directly influences the size of the segment to be generated, so that the larger its value, the larger the resulting segments. The shape plays against the spectral (or other local variable, such as DEM elevation) data. When the shape value is high, the spectral information has less important for the processing, and the increasing weight of spatial attributes tend to enhance differences in shape attributes, for example, elongation. Compactness, in opposition, concerns the contour of the segment, producing segments of smoother limits when applying lower values (BAATZ; SCHÄPE, 2000). The regionalized data of land surface parameters (LSPs) would help the delimitation of landforms in a contiguous terrain (EVANS, 1972). Considering that abrupted changes in elevation and geomorphometric variables enable the correct delineation of relief patterns, subtle changes, on the other side, may require a more difficult process in both visual and automatic classification approaches. The aim of this study consists in presenting a methodology for a hierarchical identification of landforms in Demini watershed, north of Amazonia, using regionalized LSPs. To achieve this purpose the specific goals were detailed:

- To establish a specific taxonomy for geomorphometry classes, based in BDIA'S (IBGE, 2020) Geomorphological Mapping;
- To adapt a methodology for the derivation of region-born LSPs from the terrain unit, i.e., a segment - (most of previous work computed regional data using the extension of moving windows as the terrain unit); and
- Identify the main variables for the delineation of Amazonian Highlands and Lowlands in Demini's watershed.

2. Study area

The Demini watershed is located at Barcelos municipality, in the northernmost part of Amazona's Brazilian state. It extends for nearly 40,000 square kilometers near the state of Roraima and Venezuela's frontier (Figure 1).

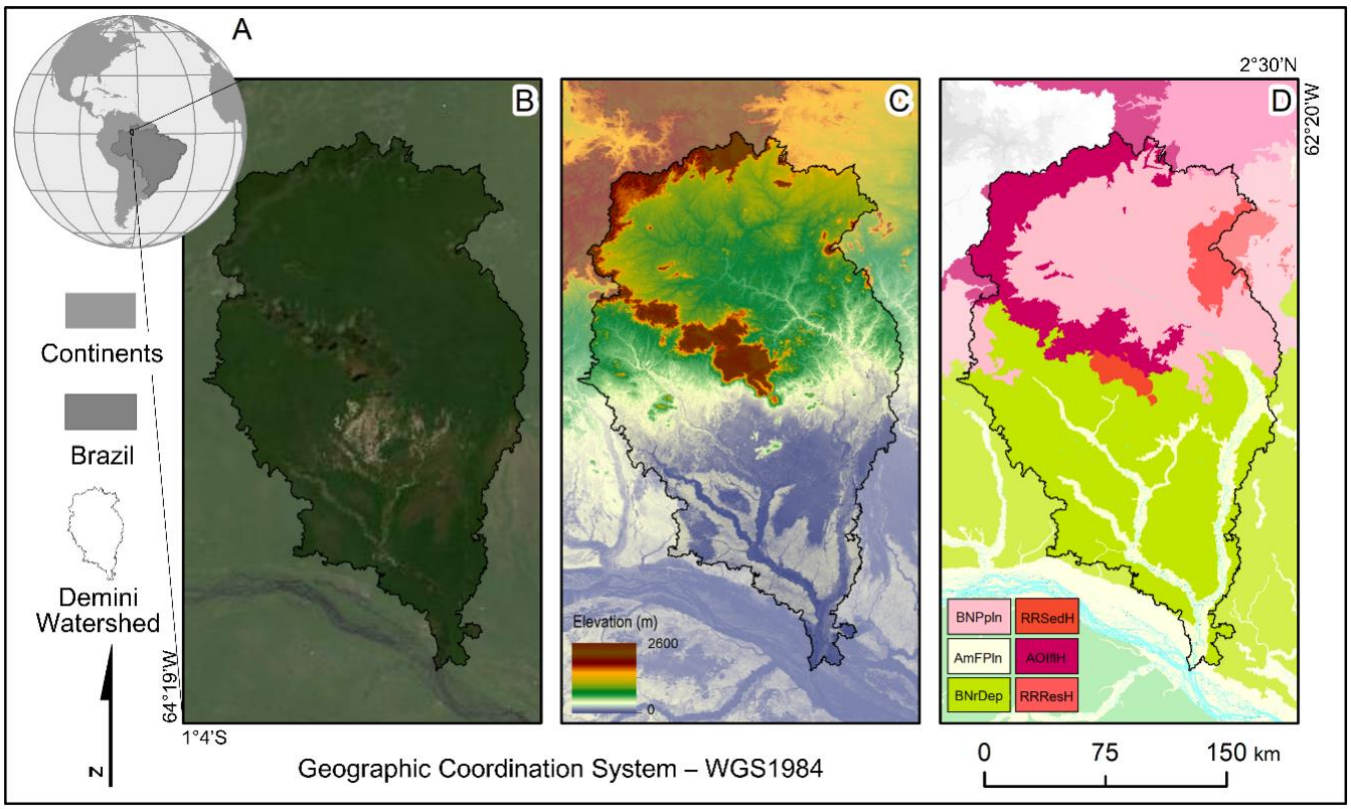

Figure 1. The Demini Watershed is localized in the north of Brazil (A). Optical remote sensing imagery, at true color composition (B), shows campinarana vegetation as bright areas among the green rainforest. Topodata DEM elevation at color scale (C), showing the same areas as low elevation depressions, contrasting with the steep hills of Guyana's shield in the central-north of the basin. IBGE's BDIA (D) has identified 6 geomorphological unities in the region's topography.

Demini's watershed has an outstanding topographic variance, with elevation values ranging from 10 to around 2500 meters. It is possible to identify different landscapes, corresponding to Amazon's highlands and floodplains (SOMBROEK, 2000). Demini's basin is a sub basin of Negro's watershed. The main tributaries that flow in Demini's basin are Araçá, Cuieiras, Tootótobi and Ananaliua rivers.

The climate is identified as tropical wet, without dry season, correspondent to "Af" type, following Koppen's classification. The annual mean air temperature is between 24 and 26 Celsius degrees. The accumulation of rainfall reaches values up to 2500 mm by year (ALVARES et al., 2013).

Vegetation in the area includes several forest and non-forest formations, including Dense and Open Ombrophilous Forest, Alluvial Open Ombrophilous Forest, Wooded Savannahs (MAPBIOMAS, 2022), Grasslands and white sand vegetation. The last one varies from open vegetation to shrub and woodlands, and are also known as *campinas* and *campinaranas* (ROSSETTI et al., 2019; IBGE, 2020). The dynamics of these are directly related to terrain's drainage (GUIMARÃES et al., 2018).

Demini's headwaters are above Precambrian igneous and metamorphic rocks of the Guyana Shield (CREMON; ROSSETTI; ZANI, 2014; ALVES; ROSSETTI; VALERIANO, 2020) where altimetry comes up to 2500 m in the highlands at north. The area presents either high altitude values in sedimentary rocks from the Roraima group, at east, presenting a specific landform type of table-top mountains, known locally as *tepuys* (IBGE, 2020), corresponding to uplifted structures. Demini's course extends then, in its mid-watershed, through the peneplain, still above Guyana shield substract, in a gently undulating surface. The river flows in this surface, with eventual

inselbergs, until reach the contact with Pantanal Setentrional, which extends in the low-watershed (IBGE, 2020; CREMON; ROSSETTI; ZANI, 2014).

Pantanal Setentrional is a sedimentary basin located northeastward of Solimões Basin, in the Amazon intracratonic rift context (ROSSETTI; MOLINA; CREMON, 2016). This area presents an extensive area of flooding, derived by tectonic activity and subsidence in the area (ALVES; ROSSETTI; VALERIANO, 2020). Through Quaternary, this area has been developed as a low plain with sediments accumulation in triangular-shaped landforms, some of which corresponding to megafan depositional systems. Demini and Viruá megafans and its hydroperiods has been documented by Rossetti et al. (2012), Zani and Rossetti (2012), and Cremon, Rossetti and Zani (2014).

3. Materials and Methods

For Demini's watershed extent and surrounding areas fourteen altimetry tiles (ZN) were obtained by the Brazilian geomorphometric database Topodata (BRASIL, 2008). These tiles, provided in tiff format, are result of an interpolation process made upon SRTM data first provided for South America, at the spatial resolution of 3 arc-second (~90m). The interpolation resulted in a DEM with 1 arc-second (~30m) side pixel, refined then for terrain analysis. Despite the availability of newer DEM of improved resolution and correction level, operational advantages of the use Topodata DEM (and the corresponding derivate layers) overwhelm the data quality gains at the scales suited for the size of study area (broader than 1:250,000), specially under the consequent regional approach.

For each data layer taken from Topodata (DEM, shaded relief and slope), the fourteen tiles were mosaicked and subsampled back to the 3 arc-second resolution (the central pixel of each 3x3 cell) to optimize storage and processing. Subsampling the derivate layers after the derivations prevents the loss of sensitivity due to lower resolution of the input DEM (VALERIANO, 2003). This first dataset was organized to serve as input during the calculation of geomorphometric variables.

Geomorphological, Geological, Soils and Vegetation maps from the Environmental Informations Database (BDIA) produced by IBGE (2019; 2020) and RADAMBRASIL (BRASIL, 1975) were used as source of general information. Besides, Landsat and Bing Maps imagery were consulted for detailed optical analysis.

The derivation of LSPs occurred accordingly its type: first, was performed the DEM-derivate, corresponding to elevation (ZN), slope (SN), terrain ruggedness index (TRI) and terrain surface texture (Text). In a second moment, the region-born variables were calculated, such as height (Alt), relative relief (RR), predominance (Pred) and dissection (Dis). The topographic predominance is a regional terrain descriptor (DENT; YOUNG, 1981) of elevation distribution, formerly conceived for photointerpretation survey. Noteworthy, the formulation for GIS estimation of regional predominance from DEM, proposed by Muñoz (2009), is the same for local topographic position given by TPI – Topographic Positional Index (WEISS, 2001). The difference between the regional and the local expressions of a same derivative must be considered, as observed for other local derivatives such as slope and profile curvature after regionalization (VALERIANO; ROSSETTI, 2017). Lastly, the derivation of LSPs was followed by the normalization of slope (nSN), height (nAlt), relative relief (nRR) and dissection (nDis), using Box-Cox transformation. The normalization process aims to reduce the effects of asymmetry and outliers in regionalization and statistical analysis of data (CSILLIK; EVANS; DRĂGUŢ, 2015).

The procedures of this research can be seen in Figure 2. The processes were performed with ArcGIS (mosaicking, subsampling, layouts, band math, rasterization, normalization); QGIS (derivation of TRI and Text); eCognition (Multiresolution segmentation); Idrisi (Trend Analysis Surface, statistics extraction) and R language (statistics extraction, charts, Random Forest).

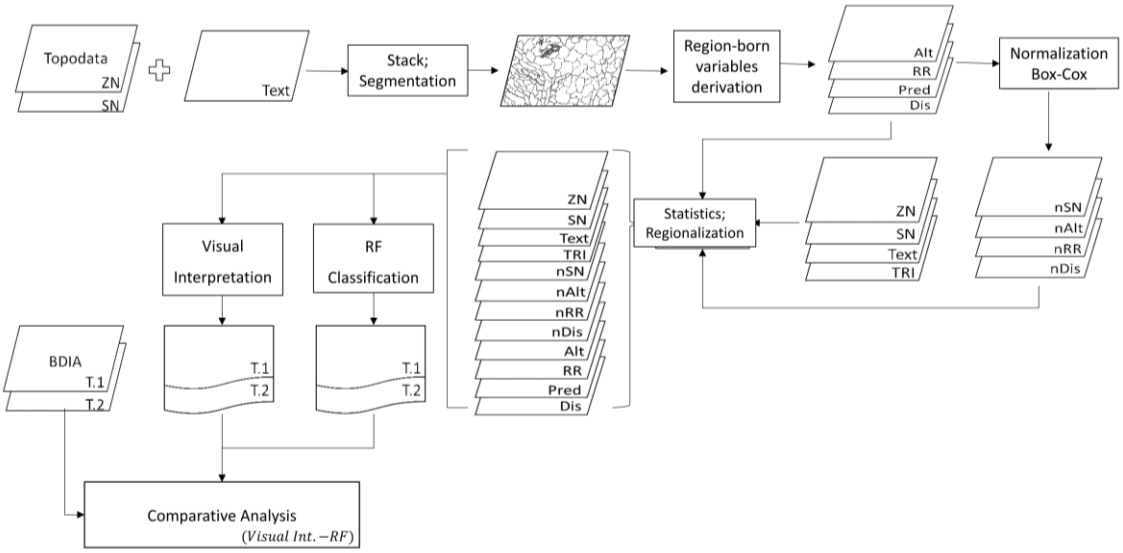

Figure 2. Methodology flowchart of this study

3.1 Derivation of land surface parameters (LSP)

The land surface parameters used in this work can be identified as DEM, DEM-derivate or Region-born variables. The DEM and Slope (SN) were obtained through TOPODATA ready-to-use database. Using Terrain and Morphometric Analysis modules implemented in SAGA GIS (CONRAD et al., 2015), the also DEM-derivate LSPs Terrain Ruggedness Index (TRI) and Terrain Surface Texture (Text) were calculated for Demini's Watershed. TRI proposes to quantify topographic heterogeneity as from the sum of differences of elevation in a 3x3 moving window (RILEY; DE GLORIA; ELLIOT, 1999). The Terrain Surface Texture is defined as the number of peaks and pits in a moving window, calculated from the differences of the original and filtered DEM (IWAHASHI; PIKE, 2007).

The Residual Relief (Res), which also consists in a DEM-derivate LSP, has been used for enhance terrain patterns in low-variated terrains, especially near fluvial plains (ZANI; ASSINE; McGLUE, 2012; VALERIANO; ROSSETTI, 2020). It was calculated as the result of a subtraction between a DEM-masked and a Trend Surface Elevation developed for the same area of the masked DEM, as in Valeriano and Rossetti (2020). The process for its acquisition can be described as: (1) chosing the corresponding area of interest for the analysis; (2) clipping the DEM for this area (ZN_{clip}); (3) calculate the Trend Surface Elevation (ZN_{trnd}) as the equation in the notation presented by Zani et al. (2012):

$$ZN_{trnd} = \sum_{i=0}^{N} \sum_{j=0}^{N} d_{ij}\, x^i y^i \tag{1}$$

where N is the polynomial degree; *i* and *j* are combining variables of interactions from 0 to N; and d is the regression coefficient; (4) set the polynomial order that best fits as a regional elevation model; (5) obtain the Residual Relief as the result of the equation:

$$Res = ZN_{clip} - ZN_{trnd} \tag{2}$$

The Trend Surface analysis was executed using TerrSet (EASTMAN, 2012), and operations of clipping and map algebra were performed with ArcGIS (Esri, 2016). Correlation of trend surface increased asymptotically with polynomial order. First and second order surfaces were suggestively fit to expected trends, considering the sedimentary environment (first order) or the bowl-model of the watershed (second order). However, from the third order on, trend surface was able to accommodate subordinate variations given by disturbances relative to these theoretical model, progressively enhancing the residues given by relative regional depressions. Thus, the residues used in this paper were taken from the ninth order trend surface. Higher order surface was not possible due to computational and software limitations.

The Region-born variables used in this research were calculated after the segmentation process, using the terrain unit (segment) as the area to perform the measurement. Height (Alt) is described as the difference between a point's elevation and the lowest measure in its surround (Equation 3). The Relative Relief, also known as the amplitude of terrain (EVANS, 1972), can be measured by subtracting the lowest value from the highest elevation in an area (Equation 4). Topographic Predominance (Pred) enhances the frequency of elevation values by subtracting the DEM mean values from the average of maximum and minimum of the computed terrain unit (5). It assumes low-predominant terrain holds isolated higher elevation values, while high-predominant areas have few lower elevation areas, probably representing terrain dissection (MUÑOZ; VALERIANO, 2014). Dissection refers to the surface lowering due to erosion. Locally, dissection may be calculated as terrain unit maxima (supposed to correspond to sediment deposition level) less the local elevation. A feasible measure of regional dissection in central Amazonia sedimentary plateaus by fluvial incision through DEM analysis (VALERIANO; ROSSETTI, 2022) was expressed as the volume of removed sediment per area within terrain units. In this paper, local expression of dissection was used as input for terrain unit characterization through regionalization after its local derivation with moving window maxima.

$$Alt = ZN - ZN_{min} \tag{3}$$

$$RR = ZN_{max} - ZN_{min} \tag{4}$$

$$\Pr e\, d = ZN - \left[\frac{(ZN_{max} + ZN_{min})}{2}\right] \tag{5}$$

Previous studies (GERENTE, 2018; ALVES, 2021) reported that the Box-Cox transformation can be applied to Slope, Height, Relative Relief and Dissection in order to transform its distribution closer to a normal (Gaussian), as suggested by Eisank et al. (2014). The procedure of normalization was carried out with the normalization toolbox developed by Csillik et al. (2015). This toolbox indicates the most appropriate exponent (in a range from –5 to 5) to reduce the asymmetry in data distribution (CSILLIK et al., 2015).

The Residual Relief (Res), which is also a DEM-derivate variable, was the last LSP to be calculated because its representation depends on setting up a specific area (ZANI; ASSINE; McGLUE, 2012). In this research, the specific area corresponds to Lowland's Taxon 1 delimitation. The low contrast in elevation values can make delineation between inundated and non-inundated areas difficult, and Res allows the enhancement of these terrain patterns.

3.2 Segmentation and regionalization of LSPs

BDIA's Geomorphological data showed the major division of relief patterns of Demini's Watershed relying on the predominance of geomorphological processes, i.e., erosion versus deposition, or, in geomorphological classification, Cratonic versus Sedimentary Domains; the ideal parameter should depict this difference. For the initial step, the first taxon landform of this classification was visually compared to LSPs DEM-derivates to assist the selection of inputs to the segmentation process and, after, the derivation of region-born variables. Although TRI and Terrain Surface Texture showed the main difference of patterns for the region's relief, Tex allowed a better visible distinction, close to BDIA's delimitation of the two main classes of the first taxon.

Once chosen as the main elements for terrain unit delineation, the DEM, Slope, and Texture layers were stacked into a single raster file. The 3-band raster was used as input for the multiresolution segmentation algorithm, implemented in eCognition software. For the first taxon, the parameters selected for this step were: Scale = 50, Shape = 0.1 and Compacity = 0.9, and all the bands had similar weights for the procedure. The same segments obtained for Taxon 1 terrain units were also used for the classification of Taxon 2 (Figure 3).

After the terrain units were established as the segments, the regionalization process started. First was made a statistical analysis of the already generated DEM-derivate LSPs, calculating the minimum, maximum, mode, mean, and range of these LSPs for each segment created. After, was calculated the region-born LSPs. This group of variables only exists considering an extent. With the segment it is possible to create these variables and, in sequence, calculate their statistics either, turning them into regionalized DEM-derivate and region-born variables.

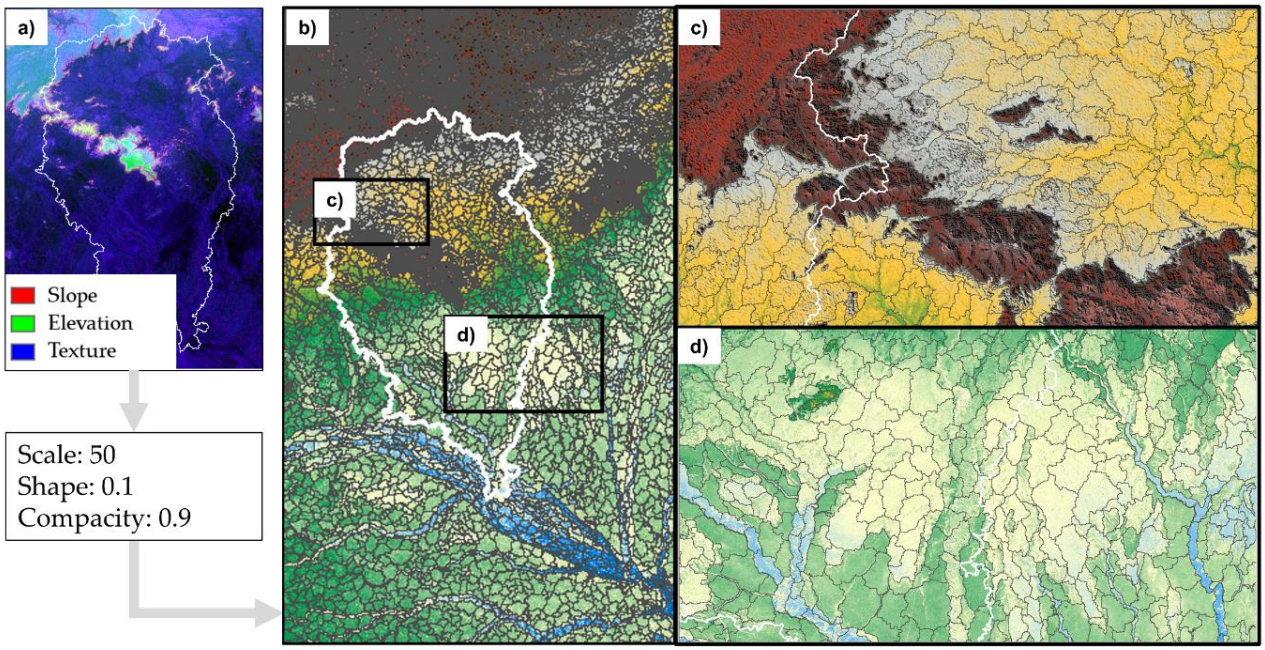

Figure 3. The segments created from the input variables (a) for the watershed region depict different patterns: smaller segments were created near to Highland (c), whereas larger segments were delineated in Lowland area (d).

Table 1. Landsurface Parameters derived for this paper using adapted methodology. They're divided by the type of derivation. DEM-derivate used only DEM and its statistics as inputs. Region-born variables comprehend LSPs that are only calculated from a given area.

LSP	Reference / Source	Type	Abbreviation
Elevation	Topodata	DEM	ZN
Slope	Topodata	DEM-derivate	SN
Normalized Slope	Topodata with toolbox	DEM-derivate	nSN
Height	Muñoz (2009) - segment	Region-born	Alt
Normalized Height	Muñoz (2009) - segment with toolbox	Region-born	nAlt
Relative Relief	Muñoz (2009) - segment	Region-born	RR
Normalized Relative Relief	Muñoz (2009) - segment with toolbox	Region-born	nRR
Terrain Surface Texture	Iwahashi and Pike (2007)	DEM-derivate	Tex
Topographic Predominance	Muñoz (2009) - segment	Region-born	Pred
Dissection	Muñoz (2009) - segment	Region-born	Dis
Normalized Dissection	Muñoz (2009) - segment with toolbox	Region-born	nDIS
Residual Relief	Valeriano and Rossetti (2017)	DEM-derivate	Res

After derivations, the maximum, minimum, mode, average, and range for each LSP were calculated using IDRISI and R for the terrain units already obtained in multiresolution segmentation.

3.3 Geomorphometric characterization of terrain units

3.3.1. Taxon 1 visual classification

The average dissection and elevation maximum were keys to delineate the limit between High and Lowland. Because values of elevation presented an abrupt break near the escarpment bordering the Sedimentary, Interfluvial, and Residual Highlands, it was important to use another LSP that would contribute dividing the

preliminary seemed "changeless" and elongated Lowland. The slicing using near escarpment values would lead to the wrong classification of peneplain in the same group of lowland. What could lead some errors in analysis for the determination of subdomains, for example, the Trend Analysis Surface derivation.

In view of the necessity of terrain classes separation by its actual processes, it was considered the Dissection as a solution to delimit Highland's Peneplain from Lowland's Plateau. The Plateau was previously characterized as slightly uneven sedimentary terrain (IBGE, 1959), and Peneplain was described as a dissected terrain with the occurrence, eventually, of inselbergs (IBGE, 2009), what led to some variations of slope, texture, and primarily, elevation and dissection (Figure 4).

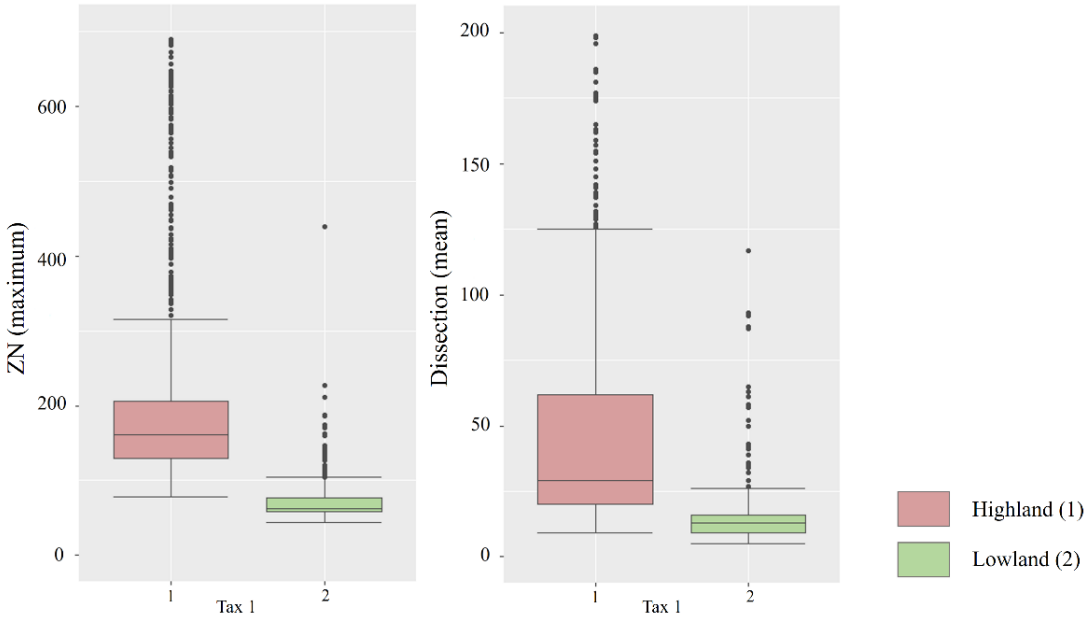

Figure 4. Boxplot of the variables used for Taxon 1 classes delineation: maximum of elevation and mean of dissection. Both were used to define Highland-Lowland limit. These boxplots were produced with random sampled points characterized from BDIA's data.

3.3.2 Taxon 2 Visual Classification

For obtaining subdomains of Highland and Lowland, the visual classification was performed for each domain individually. As shown in Figure 5.

For the Lowland was obtained a masked DEM (ZN-low) from the limit achieved in the first Taxon classification. The DEM-low was used as input for obtaining a Trend Surface Analysis (ZN-trnd), and tested some different polynomial orders, until a best fit result was found. The ZN-trnd obtained through a nineth degree polynomial had a goodness of fit (R2) of 59.32%, presenting the best result. This implies that almost 40% of regional terrain can be explained for reasons not restricted to the relief itself (its trend), and possibly tectonism and overlapping features and processes.

After the derivation of ZN-trnd, was performed the subtraction of this information from ZN-low, obtaining the Residual Relief elevation (ZN-res). ZN-res contains positive and negative values, and zero corresponds to an equitative division between positives and negatives volumes. The ZN-res was also regionalized for its analysis in a segment context. For this research area, the value of ZN-res that best fitted the delineation of Floodplains was around 1.5 (Figure 6).

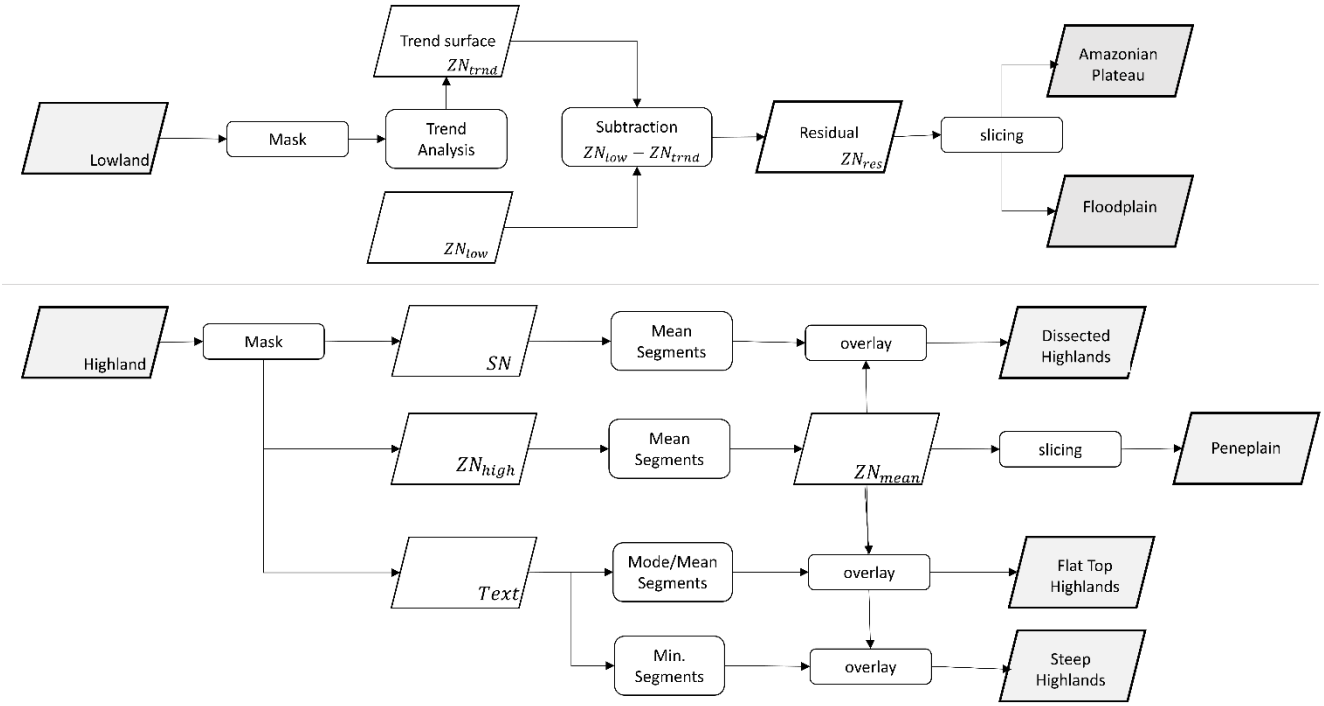

Figure 5. Classification steps using Texture, Elevation, Slope, and Residual Elevation metrics to delineate Highland's and Lowland's subdomains.

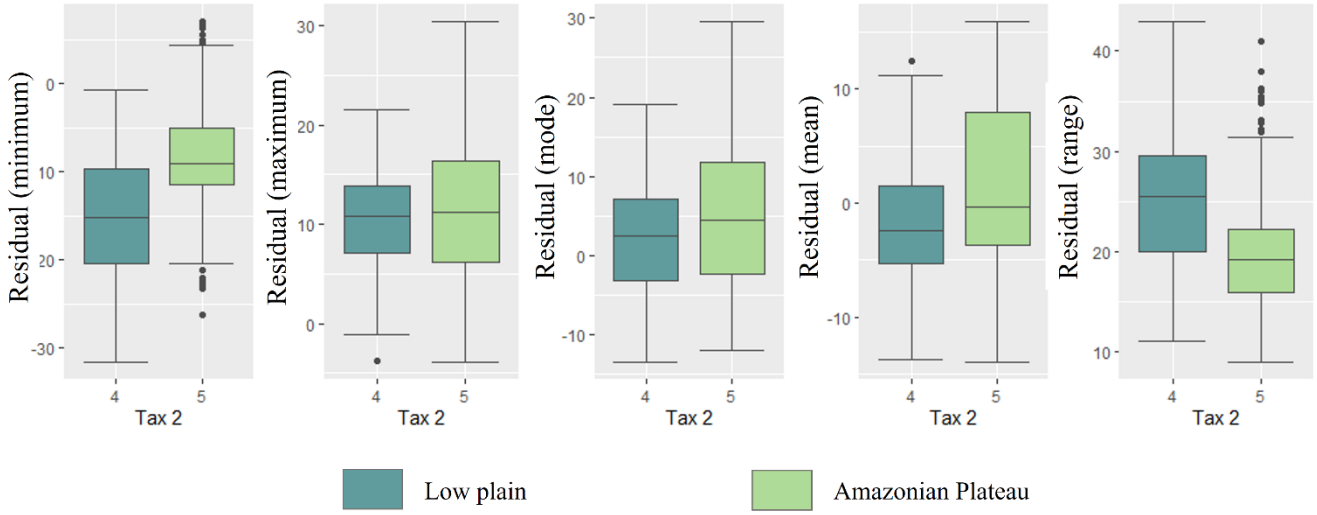

Figure 6. Boxplots of the Residual Elevation metrics obtained for random sample points of classes 4 (low plain) and 5 (Amazonian plateau).

In order to obtain Highland's subdomains, the delineation of classes followed an order. First, the Peneplain could be identified as the class with ZN mean lower than 200 meters. In sequence, the Dissected Highland was able to identify using a combination of average of ZN between 200 and 400 meters and average of slope (SN) less than 17 degrees.

The Interfluvial Highland was delineated using ZN mean higher than 420 meters, and minimum of texture above 25. The Sedimentary Highland had the same value of ZN mean set, but on the other hand, its texture values were lower than Interfluvial Highland (Figure 7).

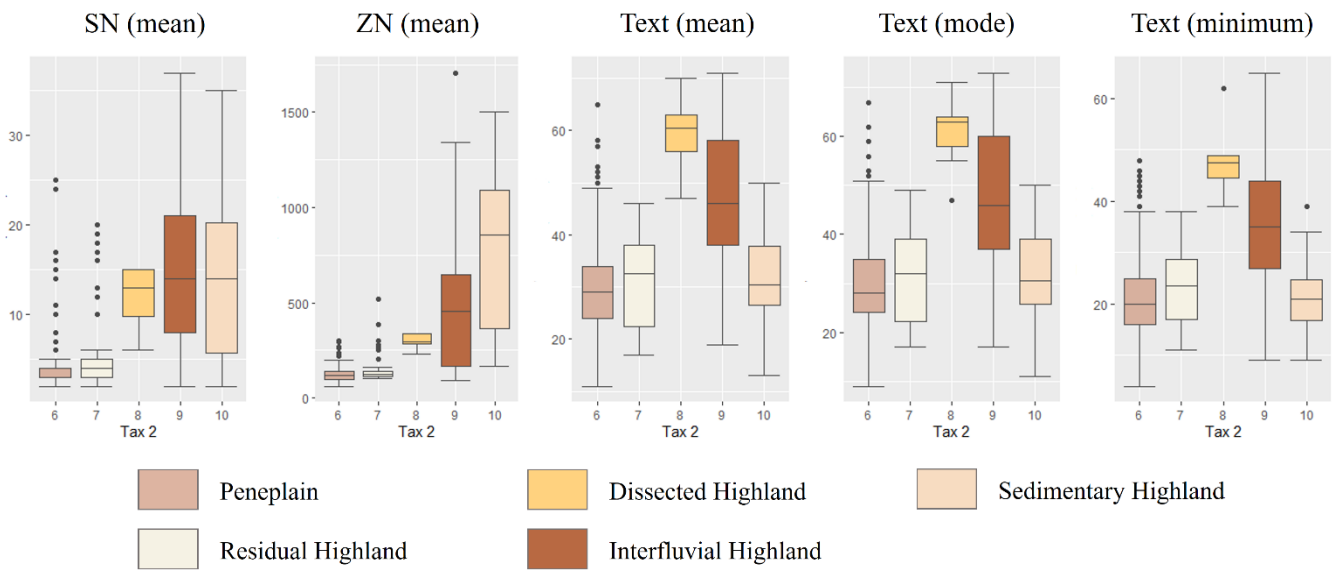

Figure 7. Boxplot of the variables used for Taxon 2's Highland classes delineation: mean of Slope (SN), mean of elevation (ZN), mean, mode and minimum of Texture. All were used to define the limits between classes 6 (peneplain), 7 (residual highland), 8 (dissected upland), 9 (interfluvial highland), 10 (sedimentary highland). These boxplots were produced with random sample points characterized from BDIA's data.

3.3.3. Random Forest Taxon 1

Random Forest is a machine learning method used for classification and regression (BREIMAN, 2001). It is based in an ensemble approach, which means it uses the result of multiple tree models combining its mode. Therefore, obtaining higher accuracy and reducing individual errors. It also allows measuring variables importance for the results.

The Random Forest (RF) classification was performed using the *randomForest* package (LIAW; WIENER, 2002), available for R language. The *ntree* parameter specifies the number of trees that will be used for the model construct. Commonly is used a large number of trees to stabilize the error of the model in its first attempts. For this research, was used the number of ntree as 500, as seen by previous works. Another parameter configured for RF is *mtry*, which specifies the number of variables selected randomly for each try. By convention, the mtry corresponds to the square root of the total number of variables used for each prediction.

The sampling process used BDIA's Geomorphological information (Morphostructural Domains) as reference for class attribution. The first step consisted in grouping BDIA'S four domains into two major classes: Cratonic and Sedimentary domains, as previously mentioned. Analyzing the area in a Geographic Information System (GIS) showed both domains had similar extents: the Cratonic Domain area corresponded to approximately 20,542 square kilometers (50.3% of the basin area), and Sedimentary Domain corresponded to approximately 20,051 square kilometers (49.07%). Water corresponds to the rest (0.63%) of the area. Thence, 1000 random sample points were extracted for each domain area, totalizing 2000 samples for the entire basin. The same samples were also identified according taxon 2 classes, with lower proportion for relief classes with smaller area representation. A minimal distance of 250 meters (nearly 3 pixels) was applied to minimize spatial autocorrelation.

For Taxon 1 RF classification, the set parameters were 70% of the 2000 random sample points (1000 for each domain) used for train and 30% for validation (Table 2), a *ntree* of 500, and a *mtry* of 7, considering the 56 prediction variables. The variables used in the model were the minimum, maximum, mode, mean, and range of the 12 LSPs listed previously, except for the minimum of Height, Dissection, normalized Dissection, and range of Relative Relief. The properties of these LSPs provided a null variance of these statistics.

Table 2. Sample point sets from Random Forest classification of the First Taxon.

Sample Summary - Taxon 1					
	Total of sample points			% Samples	
Class	**Training**	**Validation**	**Total (Class)**	**% Training**	**% Validation**
Highland	700	300	1000	0.70	0.30
Lowland	700	300	1000	0.70	0.30
Total	1400	600	2000	0.70	0.30

After first taxon classification, the resulted Highland and Lowland, relative to Cratonic and Sedimentary Domains, respectively, were separated, to identify the subdomains for each domain individually. For Lowland's Taxon 2 RF classification the set parameters were 70% of 1072 samples (from the previous 2000 set, this 1072 were inside the Lowland area) used for train and 30% for validation, a *ntree* of 500, and a *mtry* of 7, considering 61 prediction variables. This model used the previously mentioned 56 LSPs and the minimum, maximum, mode, mean and range of Residual Relief, calculated through Trend Surface Analysis performed for RF's resulted Lowland, following the already mentioned method.

Table 3. Sample point sets of Random Forest classification for random points at Lowland, Taxon 2.

Sample Summary - Lowland - Taxon 2					
	Total of sample points			% Samples	
Class	**Training**	**Validation**	**Total (Class)**	**% Training**	**% Validation**
Floodplain	105	45	150	0.70	0.30
Plateau	590	253	843	0.70	0.30
Peneplain	50	24	74	0.68	0.32
Interfluvial H.	3	2	5	0.60	0.40
Total	748	324	1072	0.70	0.30

3.3.4. Random Forest Taxon 2

For Highland's Taxon 2 RF classification the set parameters were 70% of 928 samples (from the previous 2000 set of samples, only 928 were inside the area classified as Highland) used for train and 30% for validation, a *ntree* of 500, and a *mtry* of 7, considering 56 prediction variables. In this case were used the same LSPs mentioned for the first taxon.

Table 4. Sample set of Random Forest's classification for random points at Highland, Taxon 2.

Sample Summary - Highland - Taxon 2					
	Total of samples			% Samples	
Class	Training	Validation	Total (Class)	% Training	% Validation
Plateau	5	2	7	0.71	0.29
Peneplain	383	164	547	0.70	0.30
Residual H.	49	21	70	0.70	0.30
Dissected H.	6	2	8	0.75	0.25
Interfluvial H.	188	80	268	0.70	0.30
Sedimentary H.	20	8	28	0.71	0.29
Total	651	277	928	0.70	0.30

3.4 Results analysis

The results obtained by Random Forest classification were compared with BDIA's geomorphological classes through visual analysis. The group of pixels selected as validation set during the classification process were used to obtain confusion matrix and classification metrics, such as Overall Accuracy (OA), Recall (R), Precision (P) and F1-score (F).

OA corresponds to the possibility of a pixel being correctly identified. It is calculated by dividing the sum of correctly classified pixels (true positives and true negatives) by all validation pixels (Equation 6)

$$OA = \frac{TP + TN}{TP + FP + TN + FN} \tag{6}$$

, where TP corresponds to True Positive values, TN equals to True Negative, FP means False Positive and FN is the False Negative values. R is calculated by (Equation 7)

$$R = \frac{TP}{TP + FN} \tag{7}$$

, and corresponds to how much of a class has been identified correctly by the classifier. Precision can be calculated as (Equation 8)

$$P = \frac{TP}{TP + FP} \tag{8}$$

, and means the number of correctly classified pixels divided by all the pixels the classifier has identified as the target class, wrongly or right. F1-score is calculated by the ratio between P and R using the equation 9:

$$F = 2 \times \frac{(P \times R)}{(P + R)} \tag{9}$$

, and pretends to resume precision and recall metrics into only one number.

From the randomForest package in R, the importance of variables was also calculated. The importance is measured using Mean Decrease in Accuracy (MDA), which represents the importance of the variable for each model. If a variable presents a high value of MDA, it means this variable has a high importance for the model.

In order to identify the main differences between visual and RF classifications results, visual interpretation was performed, comparing both results with each other and with BDIA's geomorphological classes. In addition, a Difference Map (DM) between classifications was also calculated, for each taxon, using the following equation:

$$DM = VC_{Tax\,N} - RFC_{Tax\,N} \tag{10}$$

, where VC corresponds to the Visual Classification result of Taxon N, and RFC is the Random Forest Classification result of the same taxon of Visual Classification being analyzed. The DM allows enhanced visualization of distinctly identified patches, emphasizing contrasts.

4. Results

The confusion matrix obtained from RF Taxon 1 (Table 5) classification detailed that the OA was 96%. The model, that considered the 56 variables (all, except the ones without variance), presented a great relationship with BDIA's data. The F1-score reached 96.2% for Highland and 96.1% for Lowland.

Table 5. Confusion Matrix of Taxon 1 validation data for random points at Random Forest classification.

Confusion Matrix				
		Reference		
		Highland	**Lowland**	**N**
Predict	**Highland**	**293**	16	309
	Lowland	7	**284**	291
	N	300	**300**	600

The metrics of RF's Highland show that the OA was 84.4%. The model also considerate the 56 variables and reached a F1-score of 89% for class 6; 55% for class 7; 80% for class 8, 81% for class 9 and 77% for class 10. In this RF Highland confusion matrix is also possible to identify samples corresponding to class number 5. These pixels were previously (in axon 1) classified as Highland but correspond to the Lowland class of Plateau.

Table 6. Confusion Matrix of Taxon 2 – Highland's validation data for random points at Random Forest classification.

Confusion Matrix								
		Reference						
		5	**6**	**7**	**8**	**9**	**10**	**N**
Predict	**5**	**0**	0	0	0	0	0	0
	6	2	**154**	12	0	14	0	182
	7	0	0	**8**	0	0	0	8
	8	0	0	0	**2**	1	0	3
	9	0	10	1	0	**65**	3	79
	10	0	0	0	0	0	**5**	5
	N	2	164	21	2	80	8	

The classification of Lowland using RF also achieved high accuracy, with OA reaching 87%, and F1-Score up to 72% for class 4 (Floodplain) and 92% for class 5 (Amazonian Plateau). For this model, 61 variables were analyzed, corresponding to the 56 mentioned before and the 5 statistics of Residual calculated for the Lowland. In the Confusion Matrix of Lowland's subdomains is also possible to identify pixels corresponding to classes 6 and 9, that were previously identified in RF's Taxon 1 as Lowland however corresponds to outcrops or isolated hills related to Peneplain and Interfluvial Highland classes.

Table 7. Confusion Matrix of Taxon 2 – Lowland's validation data for random points at Random Forest classification.

Confusion Matrix						
		Reference				
		4	**5**	**6**	**9**	**N**
Predict	**4**	**31**	10	0	0	41
	5	14	**236**	8	0	258
	6	0	7	**16**	1	24
	9	0	0	0	**1**	1
	N	45	253	24	2	

The classification obtained by visual and Random Forest classification can be seen in Figure 8, with BDIA's Geomorphological products for comparison. The maps are arranged by method of classification and corresponding taxon.

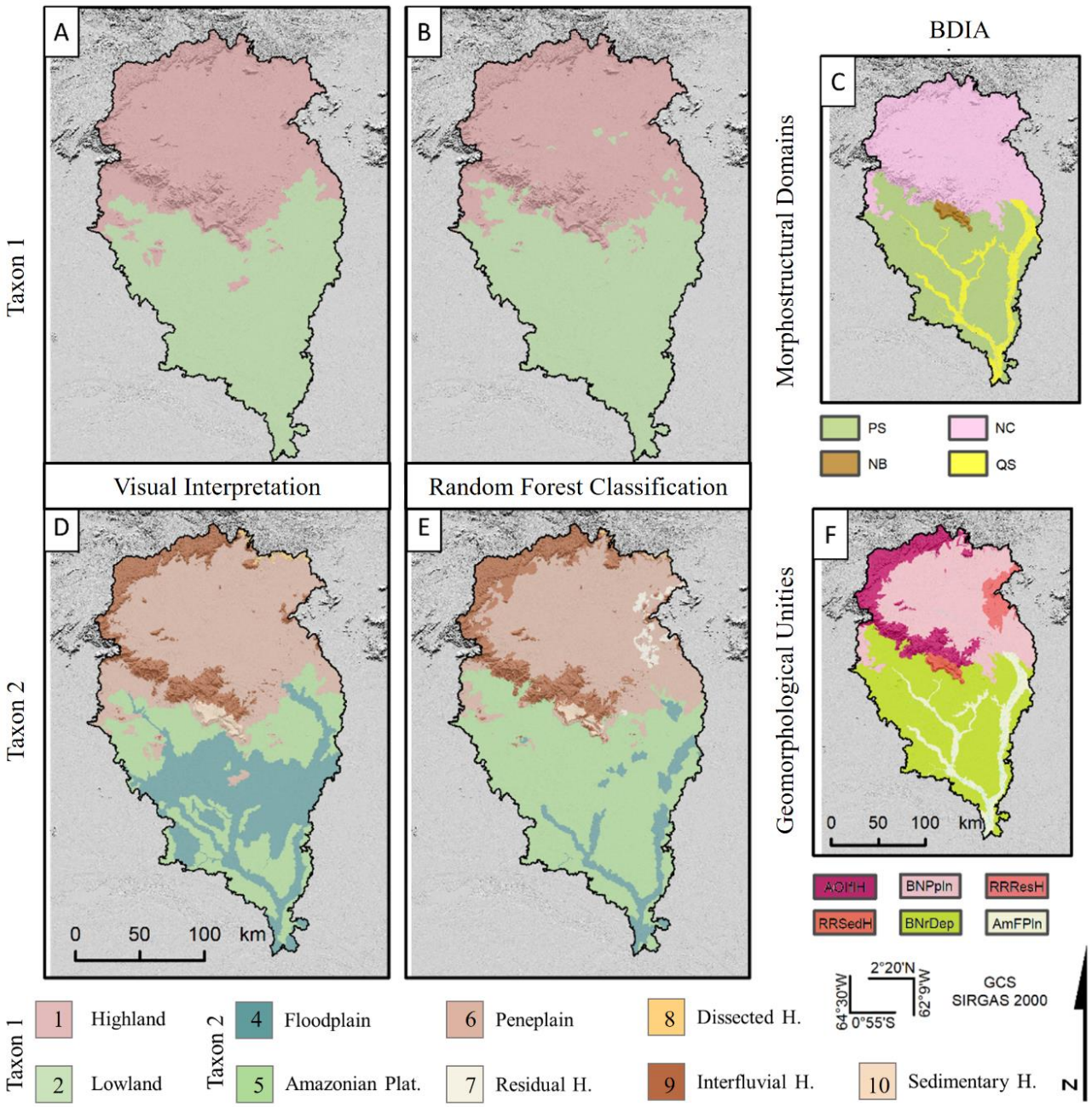

Figure 8. The classes of terrain obtained through visual interpretation (A and D), random forest classifier (B and E), and BDIA's morphostructural Domains (C) and Geomorphological Unities (F). The classes identified in A, B, D and E are: 1 (Highland), 2 (Lowland), 4 (Floodplain), 5 (Amazonian Plateau) 6 (Peneplain), 7 (Residual Highland), 8 (Dissected Highland), 9 (Interfluvial Highland), 10 (Sedimentary Highland). Figures C and F represent: PS (Phanerozoic Basins and Sedimentary covers), NB (Neoproterozoic Mobile Belts), NC (Neoproterozoic Cratons), QS (Quaternary Sediments), BNPpln (Branco-Negro Peneplain), AmFPln (Amazonian Floodplain), BNrDep (Branco-Negro Depression), RRSedH (Roraima Sedimentary Highland), AOIflH (Amazonas-Orinoco Interfluvial Highland), RRResH (Roraima Residual Highland) BDIA (IBGE, 2020).

The two grouped classes of Taxon 1 obtained through visual interpretation and RF classification presented similarities with BDIA's delineation, considering the aggregation of the 4 classes into 2. Despite a couple of lowland segments in 8.B image identified in the center of the Highland area, possibly because of low elevation values or slight variation in texture; the limits between Highland and Lowland look alike. It is also possible to identify isolated segments of Highland next to the Lowland's center in image 8.A. This area was particularly identified as Highland because of its dissection and high elevation values, which are more related to an erosional environment, distinctly from its surround.

Figure 8.E presents the same number of classes when compared with BDIA'S geomorphological units. The machine learning classifier was able to distinguish the flat top of Sedimentary Highland from the steep hills of Amazonas-Orinoco Interfluvial Highland. The Residual Highland in the area's northeastern was also identified through Random Forest, besides its delineation had been more restricted for higher terrain units, in comparison with BDIA's.

The visual interpretation of elevation, slope and texture was not capable of identifying Residual Highland in figure 8.D. However, the distinction between Sedimentary and Interfluvial Highlands were easily defined using texture's statistics. The main difference in this figure relative to the others representing Taxon 2 landforms consists in the extent of Floodplains. The Floodplains represented in BDIA's Geomorphological Unities occur adjacent to the main rivers of Demini's watershed, in its low-textured Lowland. Its identification was possible through RF especially in its lower elevation and wider areas, next to the watershed's outlet. Because of sediments accumulation that can occur in river's margins next to the Highland limit, some of these inundated segments can be identified as non-inundated areas, since its texture and slope variation increases (Fig.8.E).

The leading LSP used for visual interpretation and delineation of Lowland's subdomains was the residual of elevation, which enhanced subtle differences of height. This long extent of inundated areas was observed among the already identified Floodplains by visual classification of Res. These areas appear in contrast with its surroundings in all regionalized residual statistics, other mappings, such as vegetation, pedological and geological maps from BDIA, Amazonas Geodiversity (CPRM, 2010), and also in optical remote sensing imagery.

For a comparative analysis, the Maps of Differences (MD) were also assessed. In the first case, of Taxon 1 classifications, it's possible to visualize, through Figure 9.A, the areas of difference between classifications in bright green. These areas are concentrated in the limitation between Highland and Lowland (9.C), and occur mainly near escarpments and inselbergs (9.D; 9.E). These terrain features provide higher elevation values and discrepancies in LSPs measures on surroundings. In opposite, low patches of terrain (9.B) were identified in RF as Lowlands.

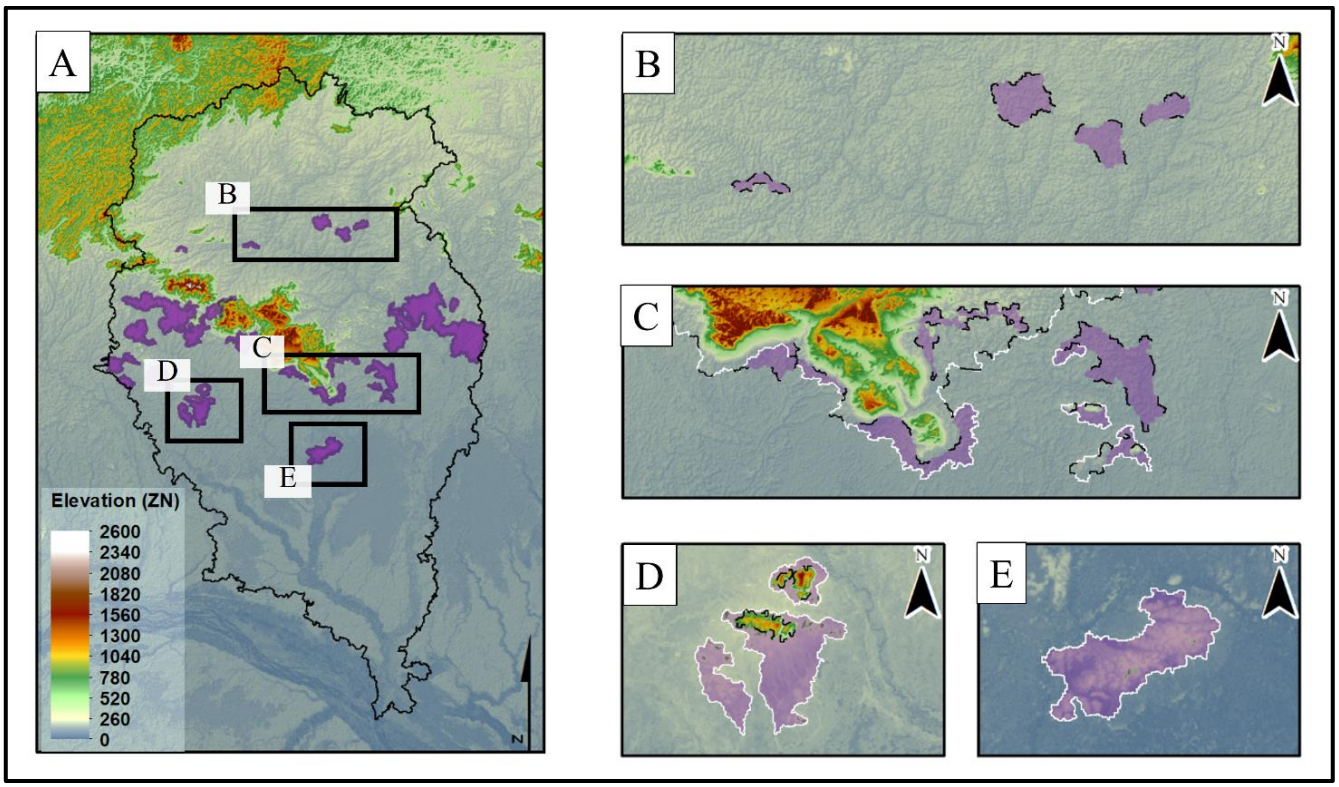

Figure 9. The Map of Differences shows in A, B, C, D, and E the main differences between the two classifications in Taxon 1 classes with the differences represented in purple. Figures B, C, D and E highlight the difference between visual and RF classification. Dashed black lines represent the class limits from the RF result, while the white line represents the limits from visual interpretation.

The MD produced for Taxon 2 classifications (Figure 10) exhibits large yellow areas, representing the main discrepancies in Demini's Watershed Terrain Mapping. Again, some incongruences appear next to Interfluvial and

Sedimentary escarpments, as seen in Figures 10.B and 10.C. Also, contrasts appear near the limits between Highland and Lowland, and mostly, in the Floodplains at south (Figure 10.D).

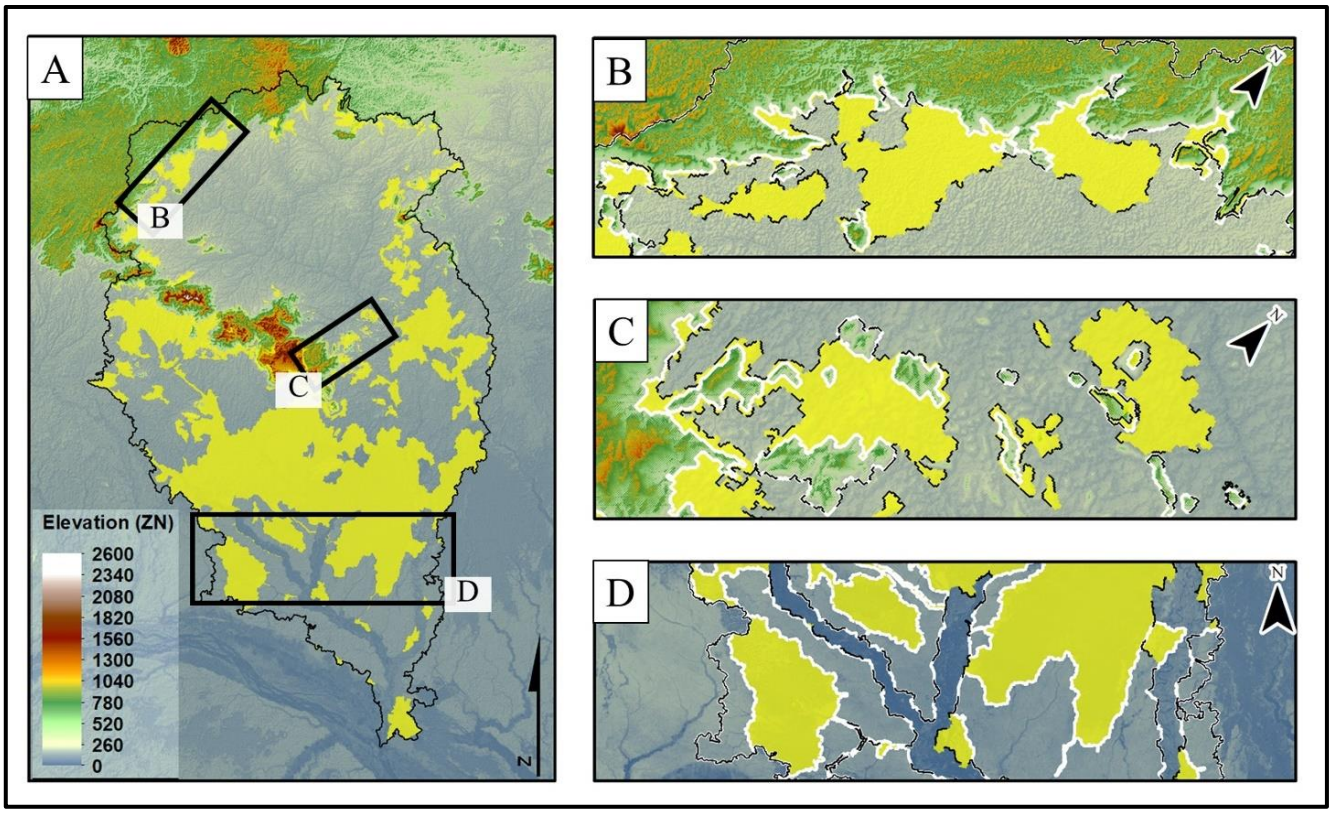

Figure 10. The Taxon 2's Map of Differences represents the variation between results in bright yellow. Figure B shows the limit between Highland and Peneplain. Figure C highlights areas close to the inselbergs in the center of the basin. And the Floodplains not considered by RF classification are seen with DEM in D. Dashed black lines represent the class limits from the RF result, the white line represents the limits from visual interpretation.

Figure 10.B shows visual classification has made a more restricted identification of the limit between Highland and Peneplain. In figure C is possible to identify a similar pattern: RF presents a broader classification if compared to VC. In figure 10.D the floodplains are highlighted in yellow, with the DEM layer overlaid by contrasts. There were also the "suspended rivers" phenomenal, that explains the differences in small patches riverside. The accumulation of sediments causes the margins to assume greater heights, which may cause doubts in the regional analysis, since these margins assume characteristics of high-predominant terrain features.

As a result of the RF classifying process, verifying the importance ranking of variables for the predictions according to the different classes is also possible. For Taxon 2 Lowland's classification was possible to identify that elevation (ZN), residual (Res), predominance (Pred) and relative relief (RR) were the most indicative variables (relative contribution above 0.02) for delineation of Floodplain and Plateau areas (Figure 11).

In Taxon 2 Highland's RF classification, the elevation (ZN) statistics plays a special role in terrain identification. Except for Dissected Highland, which has received an enormous contribution from texture (TEX) statistics, Peneplain, Residual and Sedimentary Highland had great response with ZN and predominance (Pred) data. The Interfluvial Highland, on the other hand, received great contributions from ZN, TEX and Pred for its characterization (Figure 12).

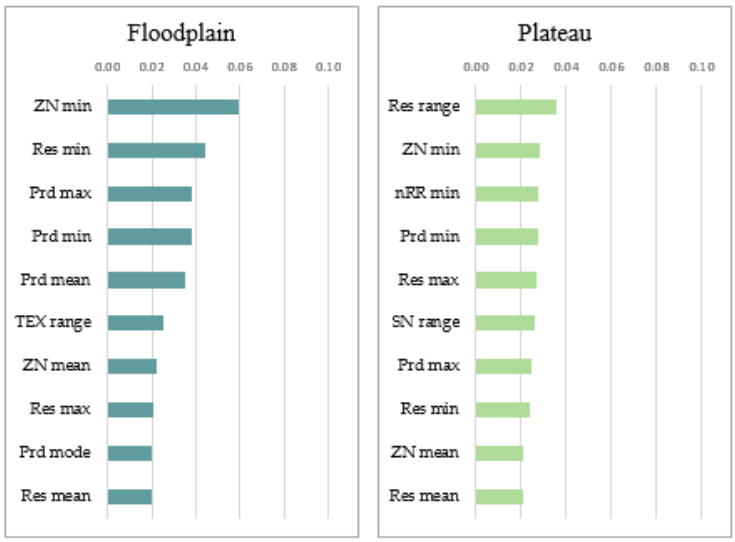

Figure 11. Ranking of variables importance for the classification of Floodplain and Plateau using Random Forest. Values close to 1 mean that the variable has higher influence on the reduction of impurity in the model.

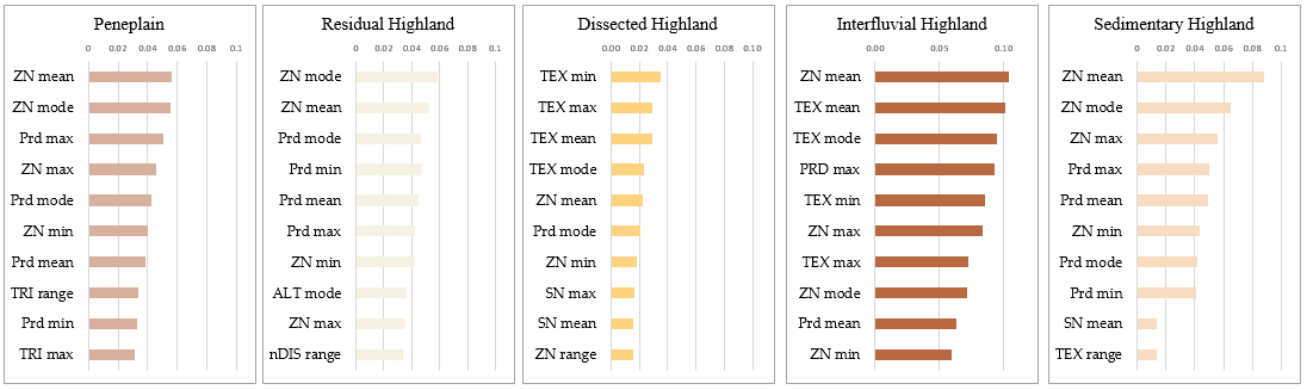

Figure 12. The graphics show the ten more important variables for the classification of Peneplain, Residual, Dissected, Interfluvial and Sedimentary Highlands using Random Forest.

5. Discussion

The Floodplain identified in the visual classification is inserted in Pantanal Setentrional Basin (ROSSETTI; MOLINA; CREMON, 2016). This sedimentary basin is a large area in northern Amazonia, where subsidence led to the accumulation of sediments during rainy seasons, and the interchangeable periods of low and high precipitation led the area to maintain a shallow wet cover. These shallow and periodically wet substract, associated with the tectonism in this area also provided an accumulation of sediments and development of megafans, with many areas completely covered with white sand (ROSSETTI et al., 2019). These areas, highlighted in Figure 10.D, were characterized by Cremon (2012) according to the frequency of inundation and associated classes of vegetation (CREMON; ROSSETTI; ZANI, 2014). Considering its flat topography, the residual of elevation provided an improvement in its delineation, as experienced by Zani, Assine and McGlue (2012) in Taquari megafan environment, and Valeriano and Rossetti (2020), in central Amazonia.

The Floodplains represented in visual classification results were identified so because of the significant amount of low residual elevation values in Branco-Negro Depression. As seen by Hess et al., (2015), Fluet-Chouinard et al. (2015), Yamazaki, Trigg and Ikeshima (2015), Pekel et al., (2016), Aires et al. (2017), Parrens et al. (2019), Rosenqvist et al. (2020) and Mapbiomas (2022) these areas can be referred to as wetlands, inundated areas, or floodplains by remote sensing products and its analysis. According to Fleischmann et al. (2022), the same areas visually classified as Floodplains have an agreement of more than 2 datasets at 1km scale identifying it as flooded areas in maximum inundation extent periods. Further studies can propose a subdivision of Floodplains in detailed

hierarchy levels. The flooded areas could be split into subgroups, such as riverside's, wedge-shaped plains, since their temporal dynamics depend on different conditions and frequencies of inundation.

BDIA's Geomorphological Mapping suited as a reference for the establishment of hierarchical arrangement of terrain features, considering the taxonomy detailed at IBGE (2009). For Demini's watershed, the first two taxons represented correspondence between reference geomorphological mapping and the geomorphometric maps resulted from this research. It implies that the establishment of a specific taxonomy following terrain processes patterns, enhanced by regionalized LSPs could delineate domains and subdomains in an area with diversified topography.

Though the present study highlights the necessity of presenting Floodplains (or wetlands) as a major feature, of a superior taxon, which has its possible subdivisions in an Amazonian Basin context, considering its extent and considerable representation. It suggests either the necessary detailed study of the Branco-Negro wetlands system and Pantanal Setentrional megafans, as well its hydroperiods and evolution dynamics.

Regionalization of LSPs allowed a well-defined result, avoiding salt and pepper effects, common in RF classification, and corresponding in a more direct way to landforms. It also enabled the analysis of homogeneity intra-segment, and the external contrasts, as mentioned by Minár and Evans (2008). Specially for Amazon's gentle topography, the regionalization provides an enhancement of patterns, and helps to minimize the canopy effect either, reducing the limitations of the SRTM data acquisition in a dense forested terrain (VALERIANO; ROSSETTI, 2017).

The use of Texture and TRI to bound Peneplain and Amazonian Plateau was proved effective. Both of these subdomains presented low elevation and slope values. However, the frequency of pits and peaks was higher in the dissected Peneplain area, allowing the delineation of these both low, but not similar dissected areas.

Most of the region-born variables used in this research were calculated in previous works using the moving windows resource (MUÑOZ; VALERIANO, 2014; MUÑOZ, 2009). Considering the segmentation result as a terrain unit itself, it was chosen to adapt the method of derivation using these segments and not moving windows, e.g. RR was calculated subtracting minimum elevation value of a segment from its maximum. This method presented suitable results for descry terrain patterns in both taxons and methodologies performed. The Mean Decrease in Accuracy method allowed the identification of the most important LSPs used for each classification model in RF. This metric enables a detailed analysis of terrain features and the process resulting in the expression of lower or higher values of the LSPs.

6. Conclusion

This paper proposed the classification of geomorphometric domains and subdomains in Demini's watershed delineating terrain features using few-steps operations in GIS software. A method of machine learning to measure importance of each LSP in the identification of terrain patterns for semi-automated techniques was also tested. The regionalization of LSPs provided effective inputs for assessment of terrain classes focusing in the homogeneity of intra-segments patterns and the surrounding contrasts.

The establishment of a hierarchical classification of domains and subdomains based in geomorphometric data enabled the development of a specific taxonomy for Demini's watershed. This methodology may contribute for delineation of terrain features in large areas such as this hydrographic basin, and in the identification of floodplains in subtle topography regions. The general steps of this mapping encompasses a structured combination of variables and processes, selected through theoretical and experimental considerations, that converges to a specific geomorphometric characterization for the existing terrains of the studied area. In addition to the general framework performance evaluation, the importance of specific variables may be noticeable for their adherence to broad conditions of Amazonian terrain, as follows.

The more important LSPs for delineation of Floodplains, Amazonian Plateau and Dissected Highland were DEM-derivate. It implies that these classes could possibly be identified using only elevation and DEM-derivate LSPs, simplifying the necessity of derivation of other variables. The most important variables used in RF model were ZN, Pred, Text, TRI and SN, and the result had similarities with BDIA's data. The main LSPs used in visual classification were the mean of ZN, SN, and Text, and also Text's mode and minimum. These LSPs provided the delineation of terrain features similarly to Geomorphological Unities, but the Residual Highland in the east was not distinguished from Interfluvial Highland characteristics by this method. The Lowland subdomain was delineated in visual classification using statistics of Res, and for the RF model this LSP had also great importance,

with ZN and Pred. The Map of Differences highlighted the big extent of flooded areas, also referred as floodplains or wetlands and suggests the representation of this terrain feature as a major landform, associated with a broader hierarchical level. Regarding this, further studies may contribute to elucidate Amazon's Floodplains evolution dynamics and processes, allowing its subdivision in narrow taxons.

Author's contributions: K.G.C.D.: Conception, Methodology, Data preparation, Formal Analysis, Research, Writing – original draft. M.M.V.: Supervision, Formal Analysis, Research, Writing – proofreading and editing. The authors read and agreed with the published version of the manuscript.

Funding: This research was developed within the master dissertation of K.G.C.D. on Remote Sensing, at the National Institute for Space Research (PGSER/DIOTG/INPE–Brazil), with scholarship of Coordination of Superior Level Staff Improvement (CAPES, process n. 88887.479685/2020-00). M.M.V. is scholarship holder of the Council for Scientific and Technological Development (CNPq, process n. 312069/2022-7).

Acknowledgments: We thank Dr. Édipo Cremon and the anonymous referees for all comments and suggestions, which effectively improved our manuscript.

Conflict of Interest: The authors declare not having any conflict of interest.

References

1. AIRES, F.; MIOLANE, L.; PRIGENT, C.; PHAM, B.; FLUET-CHOUINARD, E.; LEHNER, B.; PAPA, F. A global dynamic long-term inundation extent dataset at high spatial resolution derived through downscaling of satellite observations. **Journal of Hydrometeorology**, v. 18, n. 5, p. 1305–1325, 1 maio 2017. DOI: 10.1175/JHM-D-16-0155.1
2. ALVARES, C. A.; STAPE, J. L.; SENTELHAS, P. C.; GONÇALVES, J. S. M.; SPAROVEK, G. Köppen's climate classification map for Brazil. **Meteorologische Zeitschrift**, v. 22, n. 6, p. 711–728, 2013. DOI: 10.1127/0941-2948/2013/0507
3. ALVES, F. C. **DEM-based morphotectonic analysis of a passive continental margin of South America: Northern Paraíba Basin, NE Brazil**. Thesis—São José dos Campos: Instituto Nacional de Pesquisas Espaciais, 2021.
4. ALVES, F. C.; ROSSETTI, D. DE F.; VALERIANO, M. M. Detecting neotectonics in the lowlands of Amazonia through the analysis of river long profiles. **Journal of South American Earth Sciences**, v. 100, 1 jun. 2020. DOI: 10.1016/j.jsames.2020.102553
5. BAATZ, M.; SCHÄPE, A. Multiresolution Segmentation: an optimization approach for high quality multi-scale image segmentation. In: **Angewandte Geographische Informations-Verarbeitung**. Karlsruhe: 2001. v. XII. p. 12–23, 2001.
6. BLASCHKE, T. Object based image analysis for remote sensing. **ISPRS Journal of Photogrammetry and Remote Sensing**, v. 65, n. 1, p. 2–16, jan. 2010. DOI: 10.1016/j.isprsjprs.2009.06.004
7. BORTOLINI, W.; DA SILVEIRA, C. T. Emprego de segmentação multiresolucional no mapeamento digital de formas de relevo. **Revista Brasileira de Geomorfologia**, v. 22, n. 4, p. 899–921, 2021. DOI: 10.20502/rbg.v22i4.1987
8. BRASIL. Topodata: banco de dados geomorfométricos do Brasil. INPE, São José dos Campos: INPE, 2008. Available in: <http://www.dsr.inpe.br/topodata>
9. BRASIL, Ministério das Minas e Energia. Projeto RADAMBRASIL. Folha NA.20 Boa Vista e parte das Folhas NA.21 Tumucumaque, NB.20 Roraima e NB.21: geologia, geomorfologia, pedologia, vegetação e uso potencial da terra. Rio de Janeiro: Projeto RADAMBRASIL, 1975. 427 p. (**Levantamento de Recursos Naturais**, v. 8)
10. BREIMAN, L. Random Forests. **Machine Learning**, v. 45, p. 5–32, 2001. DOI: 10.1023/A:1010933404324
11. CASSETI, V. Cartografia Geomorfológica. **Observatório Geográfico de Goiás**, v. 20, n. 8, 2005.
12. CONRAD, O.; BECHTEL, B.; BOCK, M.; DIETRICH, H.; FISCHER, E.; GERLITZ, L.; WEHBERG, J.; WICHMANN, V.; BÖHNER, J. (2015): System for Automated Geoscientific Analyses (SAGA) v. 2.1.4, **Geosci. Model Dev.**, 8, 1991-2007, doi:10.5194/gmd-8-1991-2015. DOI: 10.5194/gmd-8-1991-2015
13. CPRM. **Geodiversidade do estado do Amazonas**. Manaus: 2010.
14. CREMON, E. H. **Caracterização morfológica do sistema fluvial do rio Demini (Amazônia Setentrional) com base em sensoriamento remoto**. Dissertação—São José dos Campos: Instituto Nacional de Pesquisas Espaciais, 2012.
15. CREMON, É. H.; ROSSETTI, D. DE F.; ZANI, H. Classification of vegetation over a residual megafan landform in the amazonian lowland based on optical and SAR imagery. **Remote Sensing**, v. 6, n. 11, p. 10931–10946, 2014. DOI: 10.3390/rs61110931
16. CSILLIK, O.; EVANS, I. S.; DRĂGUŢ, L. Transformation (normalization) of slope gradient and surface curvatures, automated for statistical analyses from DEMs. **Geomorphology**, v. 232, p. 65–77, 1 mar. 2015. DOI: 10.1016/j.geomorph.2014.12.038
17. DENT, D.; YOUNG, A. **Soil survey and land evaluation**. 1.ed. London: George Allen & Unwin, 1981. 278p.

18. DING, H.; TAO, F.; ZHAO, W.; NA, J.; TANG, G. **An object-based method for Chinese landform types classification**. International Archives of the Photogrammetry, Remote Sensing and Spatial Information Sciences - ISPRS Archives. **Anais**...International Society for Photogrammetry and Remote Sensing, 2016. DOI: 10.5194/isprs-archives-XLI-B7-213-2016
19. EASTMAN, R. **IDRISI Selva Tutorial**. Worcester: 2012. <www.clarklabs.org>.
20. EISANK, C.; SMITH, M.; HILLIER, J. Assessment of multiresolution segmentation for delimiting drumlins in digital elevation models. **Geomorphology**, v. 214, p. 452–464, 1 jun. 2014. DOI: 10.1016/j.geomorph.2014.02.028
21. ESRI Inc. **ArcMap (10.5.1)**. Redlands, United States, 2016.
22. EVANS, I. S. General Geomorphometry, derivatives of altitude, and descriptive statistics. In: CHORLEY, R. J. (Ed.). **Spatial Analysis in Geomorphology**. London: Methuen & Co., 1972. p. 17–90.
23. FLEISCHMANN, A. S.; PAPA, F.; FASSONI-ANDRADE, A.; MELACK, J. M.; WONGCHUIG, S.; PAIVA, R. C. D.; HAMILTON, S. K.; FLUET-CHOUINARD, E.; BARBEDO, R.; AIRES, F.; BITAR, A.; BONNET, M.-P.; COE, M.; FERREIRA-FERREIRA, J.; HESS, L.; JENSEN, K.; MCDONALD, K.; OVANDO, A.; PARK, E.; PARRENS, M.; PINEL, S.; PRIGENT, C.; RESENDE, A. F.; REVEL, M.; ROSENQVIST, A.; ROSENQVIST, J.; RUDORFF, C.; SILVA, T. S. F.; YAMAZAKI, D.; COLLISCHONN, W. How much inundation occurs in the Amazon River basin? **Remote Sensing of Environment**, v. 278, 1 set. 2022. DOI: 10.1016/j.rse.2022.113099
24. FLORINSKY, I. V. An illustrated introduction to general geomorphometry. **Progress in Physical Geography**, v. 41, n. 6, p. 723–752, 1 dez. 2017. DOI: 10.1177/0309133317733667
25. FLUET-CHOUINARD, E.; LEHNER, B.; REBELO, L.; PAPA, F.; HAMILTON, S. K. Development of a global inundation map at high spatial resolution from topographic downscaling of coarse-scale remote sensing data. **Remote Sensing of Environment**, v. 158, p. 348–361, 1 mar. 2015. DOI: 10.1016/j.rse.2014.10.015
26. GERENTE, J. **Aplicação de variáveis geomorfométricas ao mapeamento de padrões de relevo na bacia do rio Itajaí-Açu/SC**. Dissertação—São José dos Campos: Instituto Nacional de Pesquisas Espaciais, 2018.
27. GERENTE, J.; VALERIANO, M. M.; MOREIRA, E. P. Regionalização de variáveis geomorfométricas para o mapeamento dos domínios morfoestruturais da bacia hidrográfica do rio Itajaí-Açu (SC). **Revista Brasileira de Geomorfologia**, v. 19, n. 3, p. 433–446, 1 jul. 2018. DOI: 10.20502/rbg.v19i3.1387
28. GUIMARÃES, F. S.; BUENO, G. T.; MENDES, D. S. O.; NASCIMENTO, N. R.; DINIZ, A. D.; SOUZA, J. B. Vegetation dynamics and landscape evolution in the contact between campinarana and campina on spodosols - Demini River basin-AM (Brazil). **Revista Brasileira de Geomorfologia**, v. 19, n. 3, p. 587–600, 1 jul. 2018. DOI: 10.20502/rbg.v19i3.1288
29. HESS, L. L.; MELACK, J. M.; AFFONSO, A. G.; BARBOSA, C.; GASTIL-BUHL, M.; NOVO, E. M. L. M. Wetlands of the Lowland Amazon Basin: Extent, Vegetative Cover, and Dual-season Inundated Area as Mapped with JERS-1 Synthetic Aperture Radar. **Wetlands**, v. 35, n. 4, p. 745–756, 25 ago. 2015. DOI: 10.1007/s13157-015-0666-y
30. IBGE. **Geografia do Brasil**. Rio de Janeiro, 1959 . v. 1
31. IBGE. **Manual Técnico de Geomorfologia**. Rio de Janeiro, 2009
32. IBGE. **Macrocaracterização dos Recursos Naturais do Brasil: Províncias estruturais, compartimentos de relevo, tipos de solos e regiões fitoecológicas**. Rio de Janeiro: IBGE, 2019. 179 p.
33. IBGE. **Banco de Dados de Informações Ambientais**. V. 2.7.0. IBGE, 2020. <http://bdiaweb.ibge.gov.br/>
34. IWAHASHI, J.; PIKE, R. J. Automated classifications of topography from DEMs by an unsupervised nested-means algorithm and a three-part geometric signature. **Geomorphology**, v. 86, n. 3–4, p. 409–440, 1 maio 2007. DOI: 10.1016/j.geomorph.2006.09.012
35. KARLSON, M.; GALFALK, M.; CRILL, P.; BOUSQUET, P.; SAUNOIS, M.; BASTVIKEN, D. Delineating northern peatlands using Sentinel-1 time series and terrain indices from local and regional digital elevation models. **Remote Sensing of Environment**, v. 231, 15 set. 2019. DOI: 10.1016/j.rse.2019.111252
36. LIAW, A.; WIENER, M. Classification and Regression by randomForest. **R-news**, v. 2, n. 3, p. 18–22, 2002.
37. MAPBIOMAS. **Algorithm Theoretical Basis Document (ATBD): Collection 6**. 2022.
38. MINÁR, J.; EVANS, I. S. Elementary forms for land surface segmentation: The theoretical basis of terrain analysis and geomorphological mapping. **Geomorphology**, v. 95, n. 3–4, p. 236–259, 15 mar. 2008. DOI: 10.1016/j.geomorph.2007.06.003
39. MUÑOZ, V.A.; VALERIANO, M. M. Mapping of Flood-Plain by Processing of Elevation Data from Remote Sensing. In: PARDO-IGÚZQUIZA, E., GUARDIOLA-ALBERT, C., HEREDIA, J., MORENO-MERINO, L., DURÁN, J., VARGAS-GUZMÁN, J. (Eds). **Mathematics of Planet Earth**. Lecture Notes in Earth System Sciences. Springer, Berlin, Heidelberg, 2014. DOI: 10.1007/978-3-642-32408-6_106
40. MUÑOZ, V. A. **Análise geomorfométrica de dados SRTM aplicada ao estudo das relações solo-relevo**. Dissertação—São José dos Campos: Instituto Nacional de Pesquisas Espaciais, 2009.
41. PARRENS, M.; BITAR, A. A.; FRAPPART, F.; PAIVA, R.; WONGCHUIG, S.; PAPA, F.; YAMASAKI, D.; KERR, Y. High resolution mapping of inundation area in the Amazon basin from a combination of L-band passive microwave, optical

and radar datasets. **International Journal of Applied Earth Observation and Geoinformation**, v. 81, p. 58–71, 1 set. 2019. DOI: 10.1016/j.jag.2019.04.011

42. PEKEL, J. F.; COTTAM, A.; GORELICK, N.; BELWARD, A. S. High-resolution mapping of global surface water and its long-term changes. **Nature**, v. 540, n. 7633, p. 418–422, 15 dez. 2016. DOI: 10.1038/nature20584
43. QGIS Development Team. **QGIS Geographic Information System (version 3.16)**. 2021. Available at: <http://qgis.osgeo.org>.
44. R Core Team. R: A Language and Environment for Statistical Computing. Vienna, Áustria, 2020. Available at: <http://www.R-project.org/>.
45. RILEY, S. J.; DE GLORIA, S. D.; ELLIOT, R. A Terrain Ruggdness Index That Quantifies Topographic Heterogeneity. **Intermountain Journal of sciences** , v. 5, p. 23–27, 1999.
46. ROSENQVIST, J.; ROSENQVIST, A.; JENSEN, K.; MCDONALD, K. Mapping of maximum and minimum inundation extents in the amazon basin 2014-2017 with ALOS-2 PALSAR-2 scan SAR time-series data. **Remote Sensing**, v. 12, n. 8, 1 abr. 2020. DOI: 10.3390/rs12081326
47. ROSSETTI, D. DE F.; MOLINA, E. C.; CREMON, É. H. Genesis of the largest Amazonian wetland in northern Brazil inferred by morphology and gravity anomalies. **Journal of South American Earth Sciences**, v. 69, p. 1–10, 1 ago. 2016. DOI: 10.1016/j.jsames.2016.03.006
48. ROSSETTI, D. F.; BERTANI, T. C.; ZANI, H.; CREMON, E. H.; HAYAKAWA, E. H. Late Quaternary sedimentary dynamics in Western Amazonia: Implications for the origin of open vegetation/forest contrasts. **Geomorphology**, v. 177–178, p. 74–92, 1 dez. 2012. DOI: 10.1016/j.geomorph.2012.07.015
49. ROSSETTI, D. F.; MOULATLET, G. M.; TUOMISTO, H.; GRIBEL, R.; TOLEDO, P. M.; VALERIANO, M. M.; RUOKOLAINEN, K.; COHEN, M. C. L.; CORDEIRO, C. L. O.; RENNÓ, C. D.; COELHO, L. S.; FERREIRA, C. A. C. White sand vegetation in an Amazonian lowland under the perspective of a young geological history. **Anais da Academia Brasileira de Ciencias**, v. 91, n. 4, 2019. DOI: 10.1590/0001-3765201920181337
50. SIQUEIRA, R. G.; VELOSO, G. V.; FERNANDES-FILHO, E. I.; FRANCELINO, M. R.; SCHAEFER, C. E. G. R.; CORRÊA, G. R. Evaluation of machine learning algorithms to classify and map landforms in Antarctica. **Earth Surface Processes and Landforms**, v. 47, n. 2, p. 367–382, 1 fev. 2022. DOI: 10.1002/esp.5253
51. SOMBROEK, W. AMAZON LANDFORMS AND SOILS IN RELATION TO BIOLOGICAL DIVERSITY. **Acta Amazonica**, v. 30, n. 1, p. 81–100, 2000. DOI: 10.1590/1809-43922000301100
52. TRICART, J. **Principes et méthodes de la géomorphologie**. [s.l.] Soil Science , 1965. v. 100
53. VALERIANO, M. M. Mapeamento da declividade em microbacias com Sistemas de Informação Geográfica. **Revista Brasileira de Engenharia Agrícola e Ambiental**, v. 7, n.2, p. 303-310, 2003. DOI: 10.1590/S1415-43662003000200020
54. VALERIANO, M. M.; ROSSETTI, D. F. Regionalization of local geomorphometric derivations for geological mapping in the sedimentary domain of central Amazônia. **Computers and Geosciences**, v. 100, p. 46–56, 1 mar. 2017. DOI: 10.1016/j.cageo.2016.12.002
55. VALERIANO, M. M.; ROSSETTI, D. F. Delineation of main relief subdomains of central Amazonia for regional geomorphometric mapping with SRTM data. **Journal of South American Earth Sciences**, v. 104, 1 dez. 2020. DOI: 10.1016/j.jsames.2020.102842
56. VALERIANO, M. M.; ROSSETTI, D. F. Regional dissection volume in central Amazonia sedimentary plateau mapped from SRTM-DEM. **Journal of South American Earth Sciences**, v. 120, 2022. DOI: 10.1016/j.jsames.2022.104090
57. WEISS, A. Topographic Position and Landforms Analysis. Poster presentation, **ESRI User Conference**, San Diego, CA, 2001.
58. YAMAZAKI, D.; TRIGG, M. A.; IKESHIMA, D. Development of a global ~90m water body map using multi-temporal Landsat images. **Remote Sensing of Environment**, v. 171, p. 337–351, 15 dez. 2015. DOI: 10.1016/j.rse.2015.10.014
59. ZANI, H.; ASSINE, M. L.; MCGLUE, M. M. Remote sensing analysis of depositional landforms in alluvial settings: Method development and application to the Taquari megafan, Pantanal (Brazil). **Geomorphology**, v. 161–162, p. 82–92, 1 ago. 2012. DOI: 10.1016/j.geomorph.2012.04.003
60. ZANI, H.; ROSSETTI, D. F. Multitemporal Landsat data applied for deciphering a megafan in northern Amazonia. **International Journal of Remote Sensing**, v. 33, n. 19, p. 6060–6075, 2012. DOI: 10.1080/01431161.2012.677865